Arab J Geosci (2015) 8:2283–2298
DOI 10.1007/s12517-014-1337-7

ORIGINAL PAPER

Estimation of fundamental frequency in Dammam City, Eastern Saudi Arabia

M. Al-Malki · M. Fnais · A. Al-Amri · Kamal Abdelrahman

Received: 5 December 2013 / Accepted: 7 February 2014 / Published online: 4 March 2014

Abstract Dammam City was affected by strong earthquakes from Zagros fold-fault belt of subduction zone. These distant earthquakes of magnitude greater than 6.0 produced great site effects on the sedimentary layers that in turn significantly influenced earthquake ground motions in the area. Site effect in terms of fundamental frequency (f_0) has been estimated using microtremor measurements and borehole geotechnical data. Microtremor measurements were carried out at 113 sites distributed well through Dammam City. These sites present two peaks of f_0. The 1st peak ranges from 0.25 to 3.0 Hz, while the 2nd one ranges from 4 to 8 Hz. The 1st peak is due to the impedance contrast between the limestone and the overlying sediments, while the 2nd peak originated from the upper most surface sediments and the underlying layer. Tests to ensure that natural origin of these peaks were conducted. The northwestern and southeastern parts of Dammam City have the lowest f_0 indicating great thickness of sediments. Whereas, the rest zones have higher f_0 values illustrating shallow depths of bedrock. In addition, the geotechnical data in terms of shear wave velocity, density, and soil thickness of different layers have been compiled at 30 boreholes where f_0 and average shear wave velocities up to 30 m depth have been calculated. Results of borehole data clarified that the fundamental frequencies range between 2.9 and 7 Hz, which correlated well with that of microtremor measurements. These results can be used for land use planning, preparedness purposes through improving of building design code in Dammam City.

Keywords Fundametal frequency · Microtremor · Boreholes and building code

M. Al-Malki · M. Fnais · A. Al-Amri · K. Abdelrahman (✉)
Geology and Geophysics Department, College of Science, King Saud University, Riyadh, Kingdom of Saudi Arabia
e-mail: ka_rahmaneg@yahoo.com

K. Abdelrahman
Seismology Department, Nat. Res. Inst. of Astronomy and Geophysics, Helwan, Cairo, Egypt

Introduction

Dammam is the largest city in the eastern province of Saudi Arabia, where the judicial and administrative bodies of the province and several government departments are located in the city. In urban planning and development, the local site conditions have important implications where it controls the distribution of damages due to strong earthquakes. Many studies (Ohta et al. 1978) applied the Borcherdt's approach (1970), using ambient seismic noise instead of earthquake. This approach stated that the spectral characteristics of microtremor are associated with the site conditions (Katz 1976; Katz and Bellon 1978; Kagami et al. 1986). It became well known that with microtremors, it is possible to identify the fundamental frequency of near surface soil deposits.

Nakamura (1989) hypothesized that site response could be estimated from the horizontal to vertical spectral ratio of microtremors. This technique was tested, experimentally and theoretically, at many sites all over the world, by different authors (Bard and Tucker 1985; Ohmachi et al. 1991; Gutierrez and Singh 1992; Lermo and Chavez-Garcia 1993, 1994; Lachet and Bard 1994; Field and Jacob 1995; Malagnini et al. 1996; Teves-Costa et al. 1996; Theodulidis et al. 1996; Konno and Ohmachi 1998; Mucciarelli 1998; Mucciarelli et al. 2001; and Bard 2000). Results of Nakamura's technique support such use of microtremor measurements for estimating the site response of surface deposits. Other studies (Field and Jacob 1993; Wakamatsu and Yasui 1996; Coutel and Mora 1998; and Fnais et al. 2010) indicate

that the Nakamura method has already proved to be one of the cheapest and most convenient techniques to, reliably, estimate fundamental frequency, and it needs more work to understand the factors influencing the amplification factor.

The eastern province of Saudi Arabia (Fig. 1) suffered from, to great extent, by the active tectonics of Zagros-Bitlis subduction belts. The convergence tectonics in this area originates commonly the damaging earthquakes and represents one of the most seismically active belts (Kanamori 1986). These distant earthquakes can produce major damage in Dammam City due to local site effects. Hence, the assessment of these site effects will contribute, to great extent, in reducing the earthquake damage in this important city especially in case of increasing the population and new urban communities in this city.

Geology of Dammam City

The oldest rocks in the area are the Rus Formation exposed at the core of the Dammam dome (Fig. 2). These exposed parts represent the topmost part of the formation and consist of chalky dolomite, chalky limestone, and marl. The Dammam Formation conformably overlies the Rus Formation (Al-Sayari and Zoetl 1978). It is exposed at the edges of the Dammam dome and in small-scattered parts northwestward of the dome. It consists of dolomite, dolomitic limestone, limestone, marl, and shale. The rocks within the Dammam dome are very gently dipping and locally covered by Quaternary deposits. The Hadrukh Formation uncomfortably overlies the Dammam Formation. It consists mainly of quartz, feldspar, and calcareous materials with very small grains of chert and small quantities of anhydrite. The youngest tertiary formation in the study area is the Dam formation that unconformably overlies the Rus Formation in small part in the northwestern part of the Dammam dome.

The elevation varies from west to the east where, it ranges from 150 m at the Dammam dome to 1 m (above sea level) at the flat areas. The Dammam dome is the main geomorphologic feature through the eastern province with some hills of carbonate rocks exposures. It forms an anticlinal gently dipping structure. Sedimentary strata dip gently eastward and may interrupt locally by a series of north–south-oriented folds. A sequence of continental and shallow marine sediments extends along the Arabian Gulf with relatively low-relief terrain. The Upper Cretaceous and Eocene rocks represented by limestone and dolomite, while Quaternary sequences are composed of sandstone, sandy marl, and sandy limestone of nonmarine origin. These sequences dip gently toward the east and northeast below the thrusting of the Zagros Mountains

Fig. 1 Location map of Dammam City

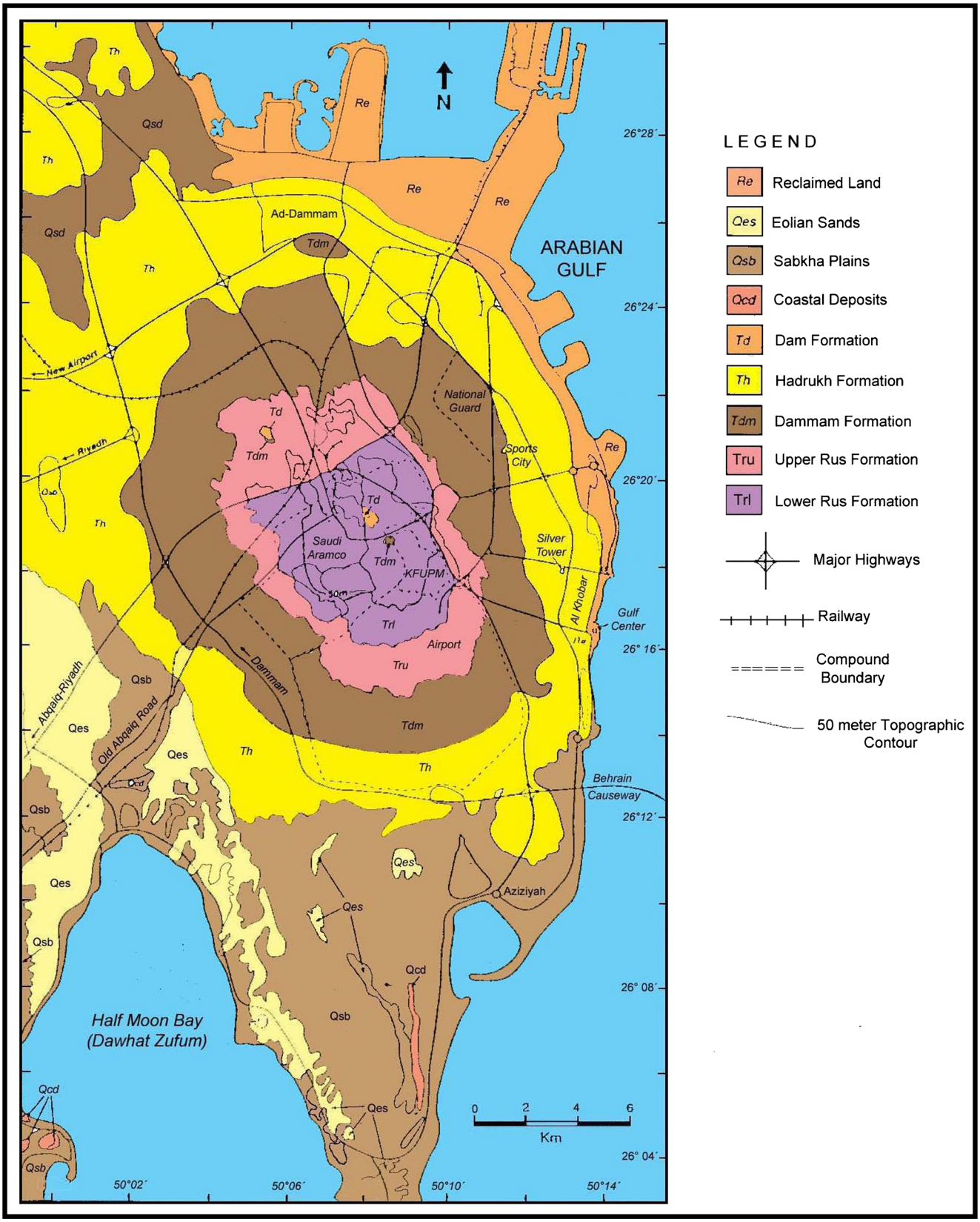

Fig. 2 Geologic map of Dammam dome (after Weijermars 1999)

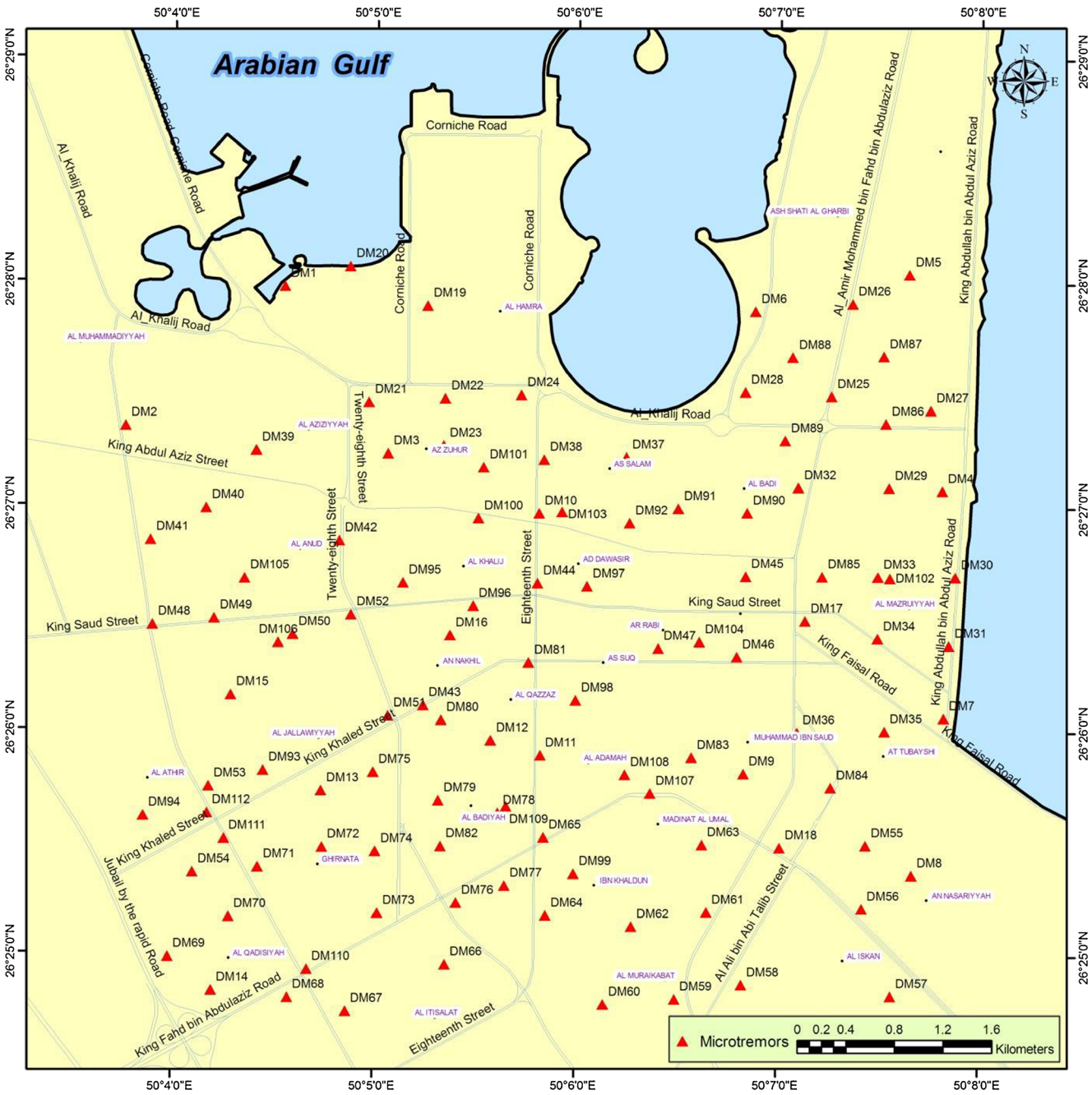

Fig. 3 Microtremor measurements in Dammam City

(Al-Sayari and Zoetl 1978). The Umm er Radhuma Formation of Paleocene and lower Eocene age forms a wide belt extending ~1,200 km from south to north with a width of 60–120 km. The exposures of the Umm er Radhuma Formation forms a gently undulating but rough surface with low altitude isolated hills and benches. Outcrops of the Dammam Formation of lower and middle Eocene age are restricted to the Arabian Gulf coastal region.

The Quaternary deposits include sabkhah, coastal deposits, surface carbonate deposits of sand and pebbles, and eolian sand. Sabkhah deposits covered by relatively thin sheet of eolian sand. The marine deposits overlie the sabkhah. Most of the marine deposits are 1 to 3 m wide from the shoreline. The surface carbonate deposits are formed in the flat areas and in the depressions within the carbonate rocks exposures. The eolian sand, exist in the form of sand dunes ranging in height between 5 and 15 m. The dominant dunes in the area are barchans, barchanoid ridges, parabolic, and dome dunes. Thin sand sheets cover large area including parts of other unit like sabkha and rocks.

Table 1 Sites of microtremor measurements in Dammam City

Site code	Latitude	Longitude	Date	Start time GMT	End time GMT	Duration (min)	Sensor type	Sampling frequency
DM1	26.4663	50.0758	10 February 2011	07:50	08:20	30	T.C.	100
DM2	26.4559	50.0627	10 February 2011	13:30	13:55	25	T.C.	100
DM3	26.4539	50.0844	10 February 2011	15:00	15:20	20	T.C.	100
DM4	26.4513	50.1302	11 February 2011	06:30	07:05	35	T.C.	100
DM5	26.4674	50.1274	11 February 2011	08:16	08:46	30	T.C.	100
DM6	26.4646	50.1147	11 February 2011	09:43	10:09	26	T.C.	100
DM7	26.4344	50.1304	11 February 2011	11:09	11:35	26	T.C.	100
DM8	26.4227	50.1278	11 February 2011	12:21	12:53	32	T.C.	100
DM9	26.4302	50.1139	11 February 2011	13:30	13:50	20	T.C.	100
DM10	26.4495	50.0969	12 February 2011	10:05	10:48	43	T.C.	100
DM11	26.4315	50.0971	12 February 2011	12:31	12:51	20	T.C.	100
DM12	26.4326	50.093	13 February 2011	06:33	07:08	35	T.C.	100
DM13	26.4288	50.079	13 February 2011	08:30	09:00	30	T.C.	100
DM14	26.4139	50.07	13 February 2011	10:00	10:25	25	T.C.	100
DM15	26.4359	50.0715	13 February 2011	11:20	11:54	34	T.C.	100
DM16	26.4404	50.0896	13 February 2011	12:35	13:00	25	T.C.	100
DM17	26.4416	50.1189	13 February 2011	14:00	14:30	30	T.C.	100
DM18	26.4247	50.1169	14 February 2011	09:00	09:31	31	T.C.	100
DM19	26.4649	50.0876	8 April 2011	05:40	06:10	30	T.C.	100
DM20	26.4678	50.0812	8 April 2011	07:11	07:41	30	T.C.	100
DM21	26.4577	50.0828	8 April 2011	13:10	13:40	30	T.C.	100
DM22	26.458	50.0891	8 April 2011	14:04	14:35	31	T.C.	100
DM23	26.4545	50.089	8 April 2011	14:58	15:28	30	T.C.	100
DM24	26.4583	50.0954	8 April 2011	17:25	17:52	27	T.C.	100
DM25	26.4583	50.121	9 April 2011	04:27	04:47	20	T.C.	100
DM26	26.4652	50.1227	9 April 2011	05:33	05:53	20	T.C.	100
DM27	26.4573	50.1292	9 April 2011	06:15	06:35	20	T.C.	100
DM28	26.4586	50.1139	9 April 2011	07:00	07:27	27	T.C.	100
DM29	26.4515	50.1258	9 April 2011	08:03	08:23	20	T.C.	100
DM30	26.4449	50.1313	9 April 2011	08:50	09:12	22	T.C.	100
DM31	26.4398	50.1308	9 April 2011	09:35	09:55	20	T.C.	100
DM32	26.4515	50.1183	9 April 2011	12:00	12:20	20	T.C.	100
DM33	26.4449	50.1249	9 April 2011	14:12	14:35	23	T.C.	100
DM34	26.4403	50.1249	9 April 2011	15:00	15:20	20	T.C.	100
DM35	26.4334	50.1255	9 April 2011	16:00	16:20	20	T.C.	100
DM36	26.4333	50.1183	9 April 2011	16:50	17:10	20	T.C.	100
DM37	26.4537	50.1041	10 April 2011	05:20	05:40	20	T.C.	100
DM38	26.4535	50.0973	10 April 2011	06:08	06:28	20	T.C.	100
DM39	26.4541	50.0735	10 April 2011	07:00	07:20	20	T.C.	100
DM40	26.4498	50.0694	10 April 2011	09:00	09:20	20	T.C.	100
DM41	26.4474	50.0648	10 April 2011	10:10	10:30	20	T.C.	100
DM42	26.4474	50.0804	10 April 2011	12:00	12:20	20	T.C.	100
DM43	26.4352	50.0874	10 April 2011	13:00	13:22	22	T.C.	100
DM44	26.4443	50.0968	10 April 2011	16:03	16:23	20	T.C.	100
DM45	26.4449	50.114	11 April 2011	05:50	06:20	30	T.C.	100
DM46	26.4389	50.1133	11 April 2011	06:48	07:18	30	T.C.	100
DM47	26.4395	50.1068	11 April 2011	07:55	08:25	30	T.C.	100
DM48	26.4411	50.065	11 April 2011	14:26	14:48	22	T.C.	100

Table 1 (continued)

Site code	Latitude	Longitude	Date	Start time GMT	End time GMT	Duration (min)	Sensor type	Sampling frequency
DM49	26.4416	50.0701	11 April 2011	15:21	15:46	25	T.C.	100
DM50	26.4404	50.0766	11 April 2011	16:15	16:35	20	T.C.	100
DM51	26.4344	50.0845	12 April 2011	05:57	06:22	25	T.C.	100
DM52	26.4419	50.0814	12 April 2011	06:45	07:09	24	T.C.	100
DM53	26.4291	50.0697	12 April 2011	09:07	09:37	30	T.C.	100
DM54	26.4227	50.0684	12 April 2011	14:52	15:02	10	T.C.	100
DM55	26.4249	50.124	11 May 2011	16:54	17:14	20	T.C.	100
DM56	26.4202	50.1237	11 May 2011	17:33	17:58	25	T.C.	100
DM57	26.4137	50.1261	11 May 2011	18:15	18:38	23	T.C.	100
DM58	26.4145	50.1138	11 May 2011	19:44	20:04	20	T.C.	100
DM59	26.4134	50.1083	12 May 2011	02:19	02:39	20	T.C.	100
DM60	26.413	50.1024	12 May 2011	03:05	03:30	25	T.C.	100
DM61	26.4199	50.1109	12 May 2011	03:57	04:22	25	T.C.	100
DM62	26.4188	50.1047	12 May 2011	04:43	05:08	25	T.C.	100
DM63	26.4249	50.1105	21 May 2011	15:50	16:10	20	T.C.	100
DM64	26.4196	50.0976	3 June 2011	16:26	16:47	21	T.C.	100
DM65	26.4254	50.0974	3 June 2011	17:10	17:30	20	T.C.	100
DM66	26.4159	50.0893	3 June 2011	17:50	18:10	20	T.C.	100
DM67	26.4114	50.0811	3 June 2011	18:25	18:45	20	T.C.	100
DM68	26.4134	50.0763	3 June 2011	19:00	19:20	20	T.C.	100
DM69	26.4164	50.0664	3 June 2011	19:40	20:00	20	T.C.	100
DM70	26.4194	50.0714	3 June 2011	20:22	20:42	20	T.C.	100
DM71	26.4231	50.0738	4 June 2011	06:15	06:35	20	T.C.	100
DM72	26.4246	50.0791	4 June 2011	06:51	07:11	20	T.C.	100
DM73	26.4197	50.0837	4 June 2011	15:30	15:50	20	T.C.	100
DM74	26.4243	50.0835	4 June 2011	16:12	16:32	20	T.C.	100
DM75	26.4302	50.0833	4 June 2011	17:04	17:24	20	T.C.	100
DM76	26.4205	50.0902	4 June 2011	17:48	18:08	20	T.C.	100
DM77	26.4218	50.0942	4 June 2011	18:30	18:50	20	T.C.	100
DM78	26.4272	50.0936	4 June 2011	19:11	19:31	20	T.C.	100
DM79	26.4281	50.0887	4 June 2011	19:50	20:10	20	T.C.	100
DM80	26.4341	50.0889	4 June 2011	20:25	20:45	20	T.C.	100
DM81	26.4384	50.0961	4 June 2011	21:06	21:26	20	T.C.	100
DM82	26.4247	50.0889	5 June 2011	13:54	14:15	21	T.C.	100
DM83	26.4341	50.1096	5 June 2011	14:37	15:00	23	T.C.	100
DM84	26.4292	50.1211	5 June 2011	15:20	15:42	22	T.C.	100
DM85	26.4449	50.1203	5 June 2011	16:06	16:26	20	T.C.	100
DM86	26.4563	50.1255	5 June 2011	16:55	17:15	20	T.C.	100
DM87	26.4613	50.1253	5 June 2011	17:38	17:58	20	T.C.	100
DM88	26.4612	50.1178	5 June 2011	18:20	18:40	20	T.C.	100
DM89	26.455	50.1172	5 June 2011	19:02	19:22	20	T.C.	100
DM90	26.4496	50.1141	5 June 2011	19:52	20:12	20	T.C.	100
DM91	26.4499	50.1084	6 June 2011	13:10	13:35	25	T.C.	100
DM92	26.4488	50.1044	6 June 2011	13:55	14:15	20	T.C.	100
DM93	26.4303	50.0742	6 June 2011	16:20	16:44	24	T.C.	100
DM94	26.4269	50.0643	6 June 2011	17:10	17:40	20	T.C.	100
DM95	26.4443	50.0857	6 June 2011	18:15	18:35	20	T.C.	100
DM96	26.4426	50.0915	6 June 2011	18:56	19:16	20	T.C.	100

Table 1 (continued)

Site code	Latitude	Longitude	Date	Start time GMT	End time GMT	Duration (min)	Sensor type	Sampling frequency
DM97	26.4441	50.1009	7 June 2011	04:00	04:20	20	T.C.	100
DM98	26.4356	50.1	7 June 2011	04:51	05:11	20	T.C.	100
DM99	26.4227	50.0999	7 June 2011	05:45	06:05	20	T.C.	100
DM100	26.4491	50.0919	7 June 2011	15:10	15:30	20	T.C.	100
DM101	26.4529	50.0923	7 June 2011	16:00	16:20	20	T.C.	100
DM102	26.4448	50.1259	8 June 2011	14:00	14:05	5	T.C.	100
DM103	26.4496	50.0988	8 June 2011	14:45	14:50	5	T.C.	100
DM104	26.44	50.1102	8 June 2011	15:30	15:35	5	T.C.	100
DM105	26.4446	50.0726	8 June 2011	17:08	17:13	5	T.C.	100
DM106	26.4398	50.0754	8 June 2011	17:35	17:40	5	T.C.	100
DM107	26.4287	50.1062	9 June 2011	14:42	14:48	6	T.C.	100
DM108	26.4301	50.1041	9 June 2011	15:05	15:10	5	T.C.	100
DM109	26.4277	50.0943	9 June 2011	15:35	15:40	5	T.C.	100
DM110	26.4155	50.0779	9 June 2011	15:55	16:00	5	T.C.	100
DM111	26.4252	50.071	9 June 2011	16:30	16:46	16	T.C.	100
DM112	26.4271	50.0696	9 June 2011	17:00	17:15	15	T.C.	100

T.C. trillium compact

Microtremor measurements

Dammam City bisected on a grid of 500×500 m, each comprising a discrete measurement site. Microtremor measurements have been acquired through the period from February to June 2011. Figure 3 illustrates the locations of 112 measuring sites. At each site, the microtremors were recorded continuously for, almost, 1 h.

The microtremors have been collected at the measuring sites with the following precautions according to Nakamura (1996); Mucciarelli et al. (2001); Mucciarelli (1998); and Bard and SESAME-Team (2005); (1) Using a 1-s (or higher) triaxial velocimeter, for analysis at periods longer than 1 s carried out measurements; (2) Avoid long external wiring, which may bring in mechanical and electronic interferences; (3) Avoid measurements in windy or rainy days. Wind causes large and unstable distortions at low frequencies; and (4) Avoid recordings close to roads with heavy vehicles, which cause strong and rather long transients.

Digital records were obtained in the range of 0.2–25 Hz band-pass filter with a sampling rate of 100 samples per second. Table 1 presents the parameters of these measurements at the various sites. The length of recording for each measurement is an important parameter, where too short a period will result in unreliable average spectral ratios. The sensors used were calibrated before recording and installed in good coupling with soil. Furthermore, it was isolated thermally against temperature changes using thick foam box and covered to reduce the interference of wind. Then, these sensors were oriented horizontally (N–S and E–W) and vertically leveled.

Borehole data

Shear wave velocity is a critical factor to identify stiffness of the sediment in determining the amplitude of ground motion (Joyner and Fumal 1984; Boore et al. 1993; Anderson et al. 1996) and might be a useful parameter to characterize local geologic conditions quantitatively for calculating site response (Tinsley and Fumal 1985; Park and Elrick 1998; Wills et al. 2000). As an alternative, the relations between shear wave velocity and several other physical properties (i.e., standard penetration test) can be identified; this can be mapped more readily on a regional scale (Fumal 1978; Fumal and Tinsley 1985). By using the method of assigning shear wave velocities to the mapped geotechnical parameters showing the engineering geologic and geotechnical parameters that correlated with shear wave velocity, such as the texture and standard penetration resistance for unconsolidated sedimentary deposits. These correlations can be applied to areal distribution, physical properties, and thickness of the geologic units to estimate and map shear wave velocity potential that is useful for seismic zonation studies. The method herein identifies soil profiles in site characterization and merges in situ measurements of dynamic properties with geologic information according to design code of ICC-IBC

(2006). Thirteen of the boreholes were conducted through Dammam City (Fig. 4). The maximum penetrated depth of these logs is about 30 m. Table 2 presents the parameters of these boreholes. SPT was performed every 1.5 m depth in every borehole according to ASTM 1992, and soil profiles and SPT blow counts are shown.

Measurements of ambient noise have been carried out very close to or directly at drilling sites where detailed information about the subsurface structure, namely the thickness of the sediments, is available. At that point, we could combine the borehole information with the observed site response functions to develop a 1-D model of the subsurface and calculate the values of S-wave velocities for the soils that characterize the investigated region.

Data processing and interpretation

Microtremor measurements

The collected data have been processed through the *Geopsy*_software developed within the framework of the great

Fig. 4 Conducted boreholes in Dammam City

Table 2 Parameters of the collected borehole data through Dammam City

Borehole no.	Name	Latitude	Longitude	Max. depth (m)	G.W.L (m)
DB1	Al Zahour School	26.4539	50.0913	6.45	3.50
DB2	Al Maarif Primary School	26.4162	50.0944	10	9.00
DB3	Yazeed Al-Shibani Primary School	26.4288	50.0880	10	
DB4	Girls' School	26.4496	50.0988	10	1.10
DB5	School	26.4342	50.0971	10	3.30
DB6	38 Primary Girls' School	26.4446	50.0726	8.5	1.20
DB7	Girls' School	26.4448	50.1259	10	1.20
DB8	General Girls' Education	26.4495	50.0969	10.5	4.50
DB9	Girls' School	26.4309	50.0742	8	1.10
DB10	Zaid Bin Al Khattab School	26.4104	50.0785	10	7.00
DB11	Intersection	26.4411	50.0650	25	0.60
DB12	Intersection	26.4251	50.1146	35	2.70
DB13	Civil Defense.	26.4301	50.1041	12	2.60

G.W.L ground water level (m)

European project SESAME. At each site, the field measurements sheet proposed by the SESAME European project (SESAME Guidelines 2004) was conducted in terms of time, date, operator name, coordinates, etc. All the necessary and recommended information about the recorded signals were applied according to these guidelines.

Criteria for reliability of results

SESAME project recommended several criteria for reliability of results as follows;

$$f_0 > 10/I_w$$

According to this condition, at the frequency of interest, there is at least ten significant cycles in each window. If the data allows, but this is not mandatory, it is always fruitful to check whether a more stringent condition (f_0>20/I_w), can be fulfilled, which allows at least ten significant cycles for frequencies half the peak frequency and thus enhances the reliability of the whole peak.

$$n_c(f_0) > 200$$

According to this condition, a large number of windows are needed. The total number of significant cycles: n_c=I_w,f_0 is larger than 200 (which means, for instance, for a peak at 1 Hz, that there are at least 20 windows of 10 s each; or, for a peak at 0.5 Hz, ten windows of 40 s each). In case no window selection is considered, (all transients are taken into account).

$$\sigma_A(f) < 2 \text{ for } 0.5f_0 < f < 2f_0 \quad \text{if } f_0 > 0.5 \text{ Hz}$$
$$\text{or } \sigma_A(f) < 3 \text{ for } 0.5f_0 < f < 2f_0 \quad \text{if } f_0 < 0.5 \text{ Hz}$$

This condition takes into account an acceptably low level of scattering between all windows.

Criteria for clear H/V peak

According to the SESAME Guidelines, at least five of the following criteria must be achieved for the clarity of H/V peaks.

$$\exists f^- \in \left[\frac{f_0}{4}, f_0\right] \left| A_{H/V}(f^-) < A_0/2 \right.$$

One frequency f^-, should be lying between f_0/4 and f_0, such as $A_0/A_{H/V}$ (f^-)>2.

$$\exists f^+ \in [f_0, 4f_0] \left| A_{H/V}(f^+) < A_0/2 \right.$$

Another frequency f^+, should be lying between f_0 and 4f_0, such as $A_0/A_{H/V}$ (f^+)>2.

$$A_0 > 2$$
$$f_{peak}\left[A_{H/V}(f) \pm \sigma_A(f)\right] = f_0 \pm 5\%$$

The peak should appear at the same frequency (within a percentage ±5 %) on the H/V curves corresponding to mean± one standard deviation.

$$\sigma_f < \varepsilon(f_0)$$

σ_f should be lower than a frequency-dependent threshold $\varepsilon(f_0)$, as in Table 3.

$$\sigma_A(f_0) < \theta(f_0)$$

$\sigma_A(f_0)$ should be lower than a frequency-dependent threshold $\theta(f_0)$, as in Table 3

Table 3 Threshold values for σ_f and $\sigma_A(f_0)$

Frequency range (Hz)	<0.2	0.2–0.5	0.5–1.0	1.0–2.0	>2.0
$\varepsilon(f_0)$ (Hz)	$0.25f_0$	$0.20f_0$	$0.15f_0$	$0.10f_0$	$0.05f_0$
$\theta(f_0)$ for $\sigma_A(f_0)$	3.0	2.5	2.0	1.78	1.58
Log $\theta(f_0)$ for $\sigma_{\log H/V}(f_0)$	0.48	0.40	0.30	0.25	0.20

where,

I_w	Window length
n_c	$I_w.n_w.f_0$ is the number of significant cycles
f_{sensor}	Sensor cutoff frequency
σ_f	Standard deviation of H/V peak frequency ($f_0 \pm \sigma_f$)
$\varepsilon(f_0)$	Threshold value for the stability condition $\sigma_f < \varepsilon(f_0)$
A_0	H/V peak amplitude at frequency f_0
$A_{H/V}(f)$	H/V curve amplitude at frequency f
$\theta(f_0)$	Threshold value for the stability condition $\sigma_A(f) < \theta(f_0)$
$V_{s,\ surf}$	S-wave velocity of the surface layer
H_{min}	Lower-bound estimate of h
n_w	Number of windows selected for the average H/V curve
f	Current frequency
f_0	H/V peak frequency
f^-	Frequency between $f_0/4$ and f_0 for which $A_{H/V}(f^-) < A_0/2$
f^+	Frequency between f_0 and $4f_0$ for which $A_{H/V}(f^+) < A_0/2$
$\sigma_A(f)$	"Standard deviation" of $A_{H/V}(f)$; $\sigma_A(f)$ is the factor by which the mean $A_{H/V}(f)$ curve should be multiplied or divided
$\sigma_{\log H/V}(f)$	Standard deviation of the log $A_{H/V}(f)$ curve; $\sigma_{\log H/V}(f)$ is an absolute value which should be added to or subtracted from the mean log $A_{H/V}(f)$ curve
$V_{s,av}$	Average S-wave velocity of the total deposits
H	Depth to bedrock

Microtremor results

At each site, the microtremor data file was divided into several time windows of 30–50 s for spectral calculations. This time window is sufficiently long to provide stable results. The selected time windows were Fourier-transformed using cosine tapering before transformation. The spectra were then smoothed with a Konno and Ohmachi algorithm (Konno and Ohmachi 1998). After data smoothing, and in order to obtain spectral ratios, the spectra of an EW and NS channels at a site were divided by the spectra of the vertical channel (Nakamura estimate). However, in most cases, due to the influence of sources from the dense population, high traffic, and various industries, the fundamental frequency cannot be directly identified from microtremor spectra (Duval et al. 2004).

Figure 5 presents average horizontal to vertical spectral ratio for this point no. 26. As shown, the dominant peak is near 7.2 Hz. The observed amplification factor is about 5. The solid line presents the average. The fundamental frequencies at all measurement sites in Dammam City are summarized in Table 4 and Fig. 6. The site response functions of the soil sites exhibit peaks at fundamental frequencies between 0.3 and 7.8 Hz. The lower f_0 values (range from 0.3 to 3.9 Hz) were attained at the northern part, while the higher f_0 values (range from 5.2 to 7.8 Hz) are presented the southern part of the study area.

The detected peaks of fundamental frequencies have tested for the industrial origin according to (Dunand et al. 2002) and the SESAME European Project Guidelines (2004).

The shapes of the empirical site response functions, as well as good agreement between both horizontal components strongly suggest that site response functions in Dammam

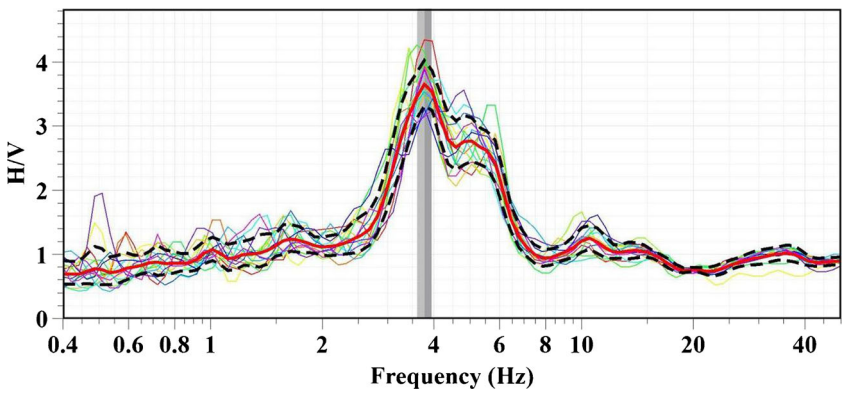

Fig. 5 HVSR spectra for DM-70 site in Dammam City

Table 4 Results of microtremor measurements of Dammam City

Site code	No. of samples	(n_w)	(I_w)	(n_c)	(A_0)	$\sigma_A(f)$	(f_0)	(σ_f)
DM1	177,184	25	50	375	3.3	1.8	0.3	0.02
DM2	150,000	16	50	2,480	2.21	1.18	3.1	0.53
DM3	120,000	12	50	3,492	2.53	1.1	5.82	0.35
DM4	210,000	10	50	1,535	1.92	1.15	3.07	0.59
DM5	180,000	11	50	2,002	2.17	1.1	3.64	0.88
DM6	156,000	19	50	4,332	2.7	1.17	4.56	0.43
DM7	156,000	14	50	4,200	2.4	1.16	6.00	0.46
DM8	191,613	12	50	618	1.48	1.35	1.03	0.07
DM9	150,000	16	50	2,480	2.22	1.19	3.10	0.53
DM10	258,000	43	50	16,770	2.66	1.12	7.8	0.35
DM11	120,000	10	15	567	1.95	1.48	3.78	0.49
DM12	210,000	18	50	3,600	1.77	1.13	4.00	0.58
DM13	180,000	15	50	2,850	2.44	1.14	3.8	0.30
DM14	150,000	12	45	2,457	3.15	1.13	4.55	0.52
DM15	203,212	10	35	1,890	2.99	1.25	5.4	0.94
DM16	150,000	18	50	3,600	2.53	1.16	4.00	0.71
DM17	180,000	12	50	3,168	3.39	1.14	5.28	0.25
DM18	180,000	10	50	670	1.79	1.19	1.34	0.17
DM19	180,000	10	30	84	5.9	1.36	0.28	0.04
DM20	180,000	10	35	105	2.00	1.7	0.3	0.06
DM21	180,000	16	50	3,984	3.67	1.1	4.98	0.42
DM22	186,000	10	40	120	2.3	1.5	0.3	0.03
DM23	180,000	10	50	135	1.8	1.4	0.27	0.02
DM24	162,000	10	40	120	3.9	2.3	0.3	0.03
DM25	120,000	10	25	1,250	3.29	1.18	5.00	0.69
DM26	120,000	10	50	2,535	3.14	1.12	5.07	0.51
DM27	120,000	13	50	1,931	2.43	1.12	2.97	0.37
DM28	162,000	10	50	2,470	3.64	1.1	4.94	0.39
DM29	120,000	10	50	1,315	2.45	1.17	2.63	0.37
DM30	132,000	10	45	126	5.5	1.5	0.28	0.03
DM31	120,000	10	45	3,492	3.1	1.25	7.76	0.73
DM32	120,000	10	50	3,305	3.32	1.2	6.61	0.63
DM33	138,000	14	50	3,626	2.79	1.15	5.18	0.31
DM34	120,000	10	25	1,430	2.86	1.16	5.72	0.51
DM35	120,000	10	40	2,060	1.9	1.1	5.15	0.82
DM36	120,000	12	50	1,020	1.25	1.13	1.7	0.087
DM37	120,000	10	35	1,337	1.07	1.09	3.82	0.09
DM38	120,000	10	50	1,315	2.55	1.17	2.63	0.61
DM39	120,000	10	45	1,373	2.61	1.27	3.05	0.34
DM40	120,000	10	50	1,710	2.76	1.09	3.42	0.19
DM41	126,000	14	50	2,401	2.29	1.2	3.43	0.43
DM42	132,000	10	35	1,225	1.68	1.13	3.5	0.14
DM43	120,000	15	50	2,633	1.71	1.17	3.51	0.28
DM44	174,840	20	50	5,030	2.63	1.09	5.03	0.43
DM45	180,000	16	50	2,232	2.15	1.1	2.79	0.24
DM46	180,000	10	50	2,000	1.46	1.11	4.00	0.1
DM47	180,000	10	50	1,960	1.56	1.13	3.92	0.09
DM48	150,000	15	50	2,528	2.85	1.12	3.37	0.28
DM49	126,124	10	50	1,950	2.69	1.11	3.9	0.51
DM50	150,000	15	50	2,978	2.8	1.16	3.97	0.35
DM51	144,000	15	50	2,783	2.42	1.17	3.71	0.42
DM52	138,000	10	50	2,155	2.45	1.18	4.31	0.39
DM53	117,655	10	40	1,780	2.92	1.08	4.45	0.55
DM54	120,000	10	50	500	1.29	1.2	1.00	0.11
DM55	150,000	10	50	825	3.05	1.2	1.65	0.038
DM56	138,000	10	40	620	1.25	1.4	1.55	0.096
DM57	120,000	10	50	165	4.2	1.2	0.33	0.05
DM58	150,000	10	50	800	1.33	1.15	1.6	0.03
DM59	120,000	10	50	3,850	4.19	1.11	7.7	0.55
DM60	150,000	10	50	2,570	2.94	1.15	5.14	0.55
DM61	150,000	13	50	3,471	2.54	1.14	5.34	0.47
DM62	150,000	14	50	3,990	3.18	1.14	5.7	0.14
DM63	120,000	10	35	1,782	1.39	1.14	5.09	0.1
DM64	126,000	20	50	5,260	2.36	1.09	5.26	0.76
DM65	120,000	19	50	4,950	0.92	1.08	5.21	0.13
DM66	120,000	10	30	1,200	1.5	1.32	4	0.1
DM67	120,000	10	50	2,930	2.88	1.07	5.86	1.17
DM68	119,130	16	50	4,000	1.9	1.1	5	0.87
DM69	120,000	15	50	2,828	3.66	1.1	3.77	0.17
DM70	120,000	13	50	2,555	2.97	1.12	3.93	0.23
DM71	120,000	10	50	2,260	2.99	1.13	4.52	0.72
DM72	120,000	13	50	3,328	2.46	1.13	5.12	0.49
DM73	120,000	14	50	3,794	2.14	1.11	5.42	0.61
DM74	120,000	14	50	3,325	1.45	1.09	4.75	0.83
DM75	119,305	18	50	4,437	2.29	1.11	4.93	0.54
DM76	120,000	15	50	3,675	1.22	1.13	4.9	0.12
DM77	120,000	16	50	3,728	2.4	1.12	4.66	0.75
DM78	117,957	13	50	3,465	2.42	1.1	5.33	0.33
DM79	120,000	11	35	1,964	2.1	1.19	5.1	0.68
DM80	120,000	13	50	2,529	2.12	1.11	3.89	0.27
DM81	120,000	10	45	1,665	2	1.13	3.7	0.51
DM82	132,000	15	50	3,795	2.32	1.11	5.06	0.16
DM83	138,000	10	45	1,395	1.77	1.16	3.1	0.37
DM84	132,000	10	50	140	3.76	1.58	0.28	0.03
DM85	120,000	10	30	1,515	2.52	1.15	5.05	0.89
DM86	120,000	10	50	1,330	3.15	1.22	2.66	0.34
DM87	120,000	10	50	1,580	3.33	1.18	3.16	0.5
DM88	120,000	14	50	3,150	3.23	1.09	4.50	0.53
DM89	120,000	13	50	3,341	3.56	1.1	5.14	0.49
DM90	120,000	14	50	2,954	3.89	1.09	4.22	0.61
DM91	150,000	10	25	1,448	2.22	1.17	5.79	0.66
DM92	120,000	10	50	2,000	1.4	1.13	4	0.1
DM93	144,000	10	50	1,860	3.08	1.09	3.72	0.22
DM94	180,000	10	50	1,910	1.63	1.16	3.82	0.54
DM95	117,105	12	50	2,220	1.52	1.11	3.7	0.49
DM96	115,629	10	35	1,341	2.8	1.15	3.83	0.24

Table 4 (continued)

Site code	No. of samples	(n_w)	(I_w)	(n_c)	(A_0)	$\sigma_A(f)$	(f_0)	(σ_f)
DM97	115,535	10	40	1,496	1.89	1.14	3.74	0.35
DM98	120,000	11	35	1,448	2.27	1.19	3.76	0.25
DM99	120,000	10	50	2,815	1.52	1.13	5.63	0.12
DM100	120,000	16	50	3,040	1.81	1.12	3.8	0.44
DM101	116,668	13	50	4,219	2.85	1.07	6.49	0.68
DM102	30,000	10	20	1,158	3.03	1.4	5.79	0.72
DM103	30,000	10	15	483	1.33	1.2	3.22	0.08
DM104	30,000	11	15	774	1.96	1.29	4.69	0.79
DM105	26,759	10	15	533	2.85	1.19	3.55	0.45
DM106	26,475	10	15	552	2.72	1.17	3.68	0.43
DM107	36,000	10	20	400	1.4	1.14	2	0.27
DM108	30,000	10	15	804	1.98	1.3	5.36	0.58
DM109	30,000	11	10	513	1.77	1.29	4.66	0.73
DM110	30,000	10	10	306	1.79	1.42	3.06	0.58
DM111	96,000	10	50	2,035	2.7	1.11	4.07	0.5
DM112	90,000	10	50	2,010	2.34	1.15	4.02	0.49

City are of 1-D nature. It is noticed that parameters of site effects are remarkably robust: Comparing two neighboring points, we found that the differences in the location of the fundamental frequencies and amplification level are small and the general shapes of the two horizontal components are similar. These findings significantly increase the reliability of the obtained information and emphasize the importance of a dense grid of observation points in microzoning studies.

Based on microtremor measurements, Dammam City divided into four zones, each characterized by a fundamental resonance frequency of the soil column as follows; $0.3 \leq f_0 < 3.9$; $3.9 \leq f_0 < 5.2$; $5.2 \leq f_0 < 6.5$; and $6.5 \leq f_0 \leq 7.8$ Hz.

Borehole results

Recent seismic code provisions have adapted site classification using average shear wave velocity and standard penetration results in the upper 30 m of a site as the sole parameter for site classification (Borcherdt 1994; Borcherdt and Glassmoyer 1994; Dobry et al. 2000; Parolai et al. 2002). The site

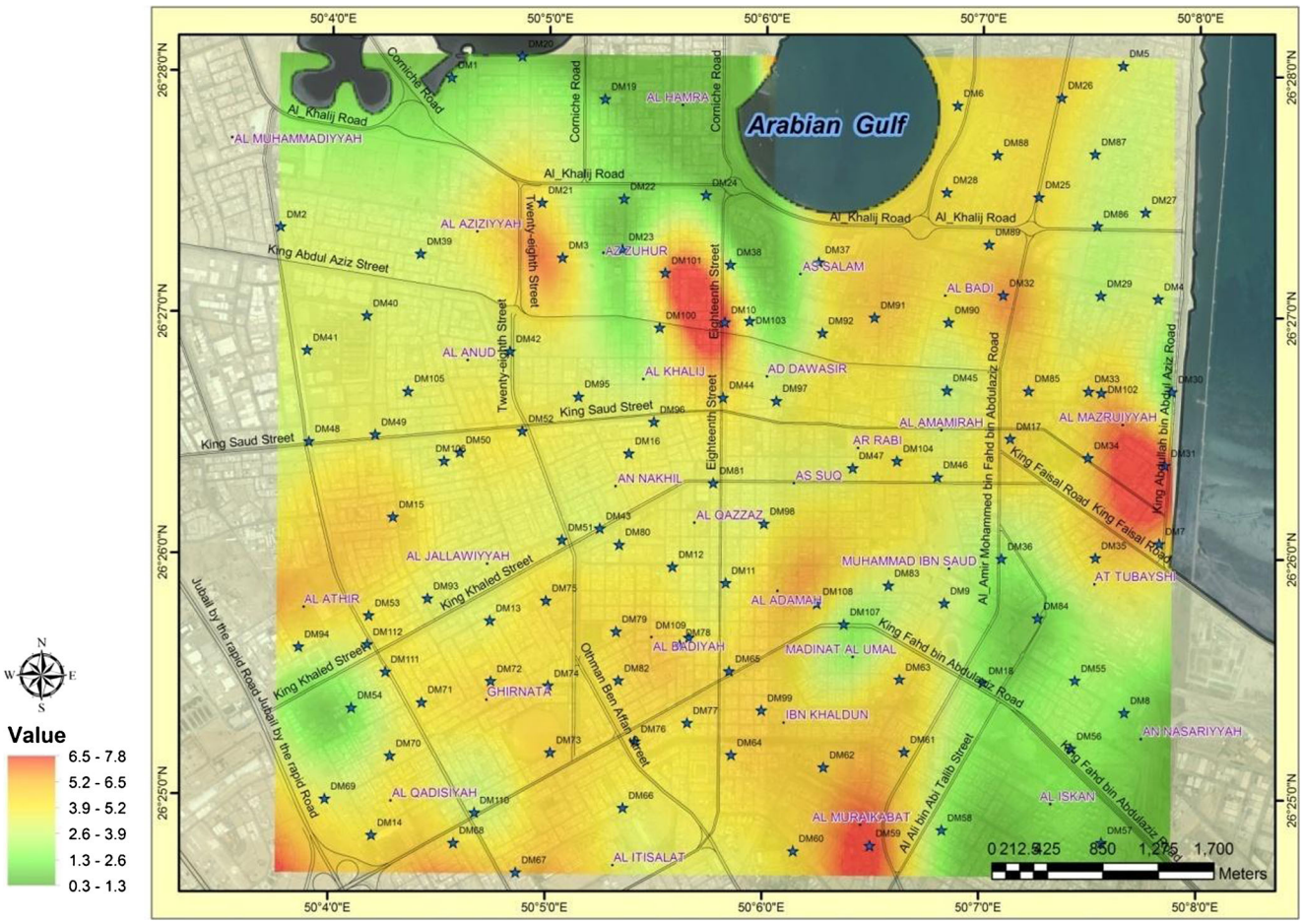

Fig. 6 Distribution of the fundamental frequencies in Dammam City

Table 5 IBC 2006 site class definitions using the average shear wave velocity and the average standard resistance to 30 m (ICC-IBC 2006)

Site class	Soil profile name	shear wave velocity, V_s (m/s)	Standard penetration resistance, N (blows/0.3 m)
A	Hard rock	V_s>1,500	N/A
B	Rock	760<V_s≤1,500	N/A
C	Very dense soil and soft rock	360<V_s≤760	N>50
D	Stiff soil profile	180<V_s≤360	15<N≤50
E	Soft soil profile	V_s<180	

conditions specified by ICC-IBC 2006 (Table 5) are identical to the provisions of IBC 2003 and practically distinguish soil profiles in the five main categories. Each category is assigned factors appropriate for the site conditions. The average shear wave velocity and correlated index measurements of the average standard penetration resistance to 30 m [(V_s (30) and N (30)] have been calculated in accordance with the following equations and then used to develop categories for local site conditions.

$$V_s(30) = \frac{\sum_{i=1}^{n} d_i}{\sum_{i=1}^{n} \frac{d_i}{V_{si}}} \qquad N\,(30) = \frac{\sum_{i=1}^{n} d_i}{\sum_{i=1}^{n} \frac{d_i}{N_i}}$$

Where V_{si} is the shear wave velocity (m/s), N_i is the standard penetration resistance (ASTM 1992) not exceeding 100 blows/0.3 m as directly measured in the field without corrections, and d_i is the thickness of any layer between 0 and 30 m.

Thirteen boreholes have been conducted through Dammam City including the values of standard penetration resistance for different depths (Table 6). Then, the standard penetration tests have been corrected for field testing where, corrections for test results to compensate the testing procedure were applied according to the following equation:

$$N_{60} = 1.6 E_m C_b C_r N$$

where,

N_{60} Standard penetration test N value corrected for field testing procedures.
E_m Hammer efficiency (for US equipment, E_m is 0.6 for a safety hammer and 0.45 for a doughnut hammer).
C_b Borehole diameter correction (C_b=1.0 for boreholes of 65–115-mm diameter, 1.05 for 150-mm diameter, and 1.15 for 200-mm diameter holes).
C_r Rod length correction (C_r=0.75 for up to 4 m of drill rods, 0.85 for 4 to 6 m of drill rods, 0.95 for 6 to 10 m of drill rods, and 1.0 for drill rods in excess of 10 m).
N Measured standard penetration test N value.

Then, the shear wave velocity has been calculated using the extrapolation method entitled "extrapolation assuming constant velocity" as proposed by Boore (2004) for boreholes that did not reach down to a depth of 30 m. Accordingly, the values of shear wave velocities ranges from 200 to 500 m/s (Table 6).

After calculation of shear wave velocities, the peaks of the fundamental frequency (f_0) is related to the surface layers both thickness and velocities. Peaks of these frequencies can be calculated using the following equation (Bard 2007):

$$f_0 = \frac{\beta_1}{4h}$$

where,

β_1 The shear wave velocity in the surficial layer
h The thickness of the surficial layer

Table 6 Results of the collected borehole data in the Dammam City

Borehole no.	Name	V_{av}	V_{30}	f_0 (Hz)	NEHRP-class
DB1	Al Zahour School	171	200	4.0	D
DB2	Al Maarif Primary School	267	500	4.6	D
DB3	Yazeed Al-Shibani Primary School	240	365	5.0	C
DB4	Girls' School	213	375	3.6	D
DB5	School	310	273	3.8	D
DB6	38 Primary Girls' School	194	448	3.6	C
DB7	Girls' School	218	316	5.7	D
DB8	General Girls' Education	284	436	7.0	C
DB9	Girls' School	192	250	3.8	D
DB10	Zaid Bin Al Khattab School	256	435	5.4	C
DB11	Intersection	177	380	3.5	C
DB12	Intersection	206	353	2.8	D
DB13	Civil Defense.	186	313	5.0	D

V_{av} shear wave velocity, f_0 fundamental frequency

Accordingly, f_0 at these boreholes are presented in Table 6 and Fig. 7. Accordingly, Dammam City has been categorized into four zones as follows: $2.9 \leq f_0 \leq 3.9$; $4.0 \leq f_0 \leq 5.1$; $5.2 \leq f_0 \leq 6.3$; and $6.4 \leq f_0 \leq 7.0$;

Conclusions

Estimation of the fundamental frequency has been applied as an aid to perform earthquake hazard microzoning in intensely populated city of Dammam. One hundred twelve measurements of microtremors were carried out to produce map of the fundamental frequency of site response. The horizontal to vertical spectral ratios obtained from microtremors proved valuable tool determine frequencies for deep and shallow soft soils with multilayer distribution and linear behaviors. There is a good correlation between results of microtremor and borehole geotechnical data (Table 7). Furthermore, the fundamental frequencies determined in the present study correlated well with the thickness of the sediments in Dammam City. These sediments are deeper on the northern part and some localized parts at the central part (site response spectra exhibit peaks at 0.3–3.9 Hz), while they are shallower on the southern part and certain areas through the city (predominant frequency of site response at 5.2–7.8 Hz). This indicate that the city vary, horizontally, in the thickness and type of sediments.

Table 7 f_0 from microtremor and borehole data

Zone no.	Microtremor measurements (Hz)	Borehole measurements (Hz)
Zone_1	0.3–3.9	2.8–3.9
Zone_2	3.9–5.2	3.9–5.1
Zone_3	5.2–6.5	5.2–6.3
Zone_4	6.5–7.8	6.4–7.0

Results of microtremor measurements indicate that reflect the ability of the Nakamura method for microzoning studies for the densely populated cities. Fundamental frequency for Dammam City can help state and local governments to set priorities in managing land use, enforcing building codes, conducting programs for reducing the vulnerability of existing structures, and planning for emergency response and long-term recovery.

Fig. 7 The fundamental frequency in Dammam City from borehole data

Acknowledgments This research was supported by NPST program by King Saud University project number 08-SPA239-2

References

Al-Sayari SS, Zoetl JG (eds) (1978) Quaternary period in Saudi Arabia. 1. Sedimentological, hydrogeological hydrochemical, geomorphological and climatological investigations in central and eastern Saudi Arabia. Springer- Verlag, Vienna

Anderson JG, Lee Y, Zeng Y, Day S (1996) control of strong motion by the 30 meters. Bull Seismol Soc Am 86(6):1749–1759

American Society for Testing and Materials (1992) Standard test method for Penetration Test and split-Barrel sampling of soils. ASTM D 1586, Vo.04 (08), Philadelphia

Bard PY (2000) International Training Course on: Seismology, Seismic Data Analysis, Hazard Assessment and Risk Mitigation Potsdam, Germany, 01 October to 05 November 2000

Bard PY (2007) International Training Course on: Seismology, Seismic Data Analysis, Hazard Assessment and Risk Mitigation, Potsdam, Germany, 07 July to 08 September 2007, pp 17–22

Bard PY, SESAME-Team (2005) Guidelines for the implementation of the H/V spectral ratio technique on ambient vibrations - measurements, processing and interpretations. SESAME European research project EVG1-CT-2000-00026 D23.12.

Bard PY, Tucker BE (1985) Underground and ridge and site effects: comparison of observation and theory. Bull Seismol Soc Am 75: 905–922

Boore DM (2004) Estimating $V_s(30)$ (or NEHRP Site Classes) from shallow velocity models (depths<30 m.). Bull Seismol Soc Am 94(2):591–597

Boore DM, Joyner WB, Fumal TE (1993) Estimation of response spectra and peak acceleration from western North American earthquakes: an interim report. US geological survey open-file report 93–509, p 72

Borcherdt RD (1970) Effects of local geology on ground motion near San Francisco Bay. Bull Seismol Soc Am 60:29–61

Borcherdt RD (1994) Estimates of site-dependent response spectra for design (methodology and justification). Earthq Spectra 10:617–653

Borcherdt RD, Glassmoyer G (1994) Influences of local geology on strong and weak ground motions in the San Francisco Bay region and their implications for site-specific building-code provisions. In: Borcherdt, R.D. (ed.): The Loma Prieta, California, earthquake of 17 October 1989-strong ground motion. US Geological Survey Prof.pap. 1551-A-:77–108

Coutel F, Mora P (1998) Simulation-based compatison of four-site response estimation technique. Seismol Soc Am 88:30–42

Dobry R, Borcherdt RD, Course CB, Idriss IM, Joyner WB, Martin GR, Power MS, Rinne EE, Seed RB (2000) New site coefficients and site classification system used in recent building seismic code provisions. Earthq Spectra 16:41–68

Dunand F, Bard, PY, Chatelain JL, Guéguen Ph, Vassail T, Farsi MN (2002) Damping and frequency from random method applied to in-situ measurements of ambient vibrations: evidence for effective soil structure interaction. 12th European Conference on Earthquake Engineering, London. Paper# 869

Duval AM, Chatelain JL, Guillier B, SESAME Project WP02 Team (2004) Influence of experimental conditions on H/V determination using ambient vibrations (noise). Proceedings of the 13th World Conference on Earthquake Engineering, Vancouver, August 2004, paper # 306

Field E, Jacob KH (1993) The theoretical response of sedimentary layers to ambient seismic noise. Geophys Res Lett 20(24):2925–2928

Field EH, Jacob KH (1995) A comparison and test of various site-response estimation techniques, including three that are not reference-site dependent. Bull Seismol Soc Am 85:1127–1143

Fnais MS, kamal Abdelrahman, Al-Amri AM (2010) Microtremor measurements in Yanbu City of western Saudi Arabia: a tool of seismic microzonation. J King Saudi Univ Sci. doi:10.1016/j.jksus.2010.02.006

Fumal TE (1978) Correlations between seismic wave velocities and physical properties of near-surface geologic materials in the southern San Francisco Bay region, California. US Geological Survey Open-file Report 78–1067

Fumal TE, Tinsley JC (1985) Mapping shear-wave velocities of near-surface geologic materials, US Geological Survey Prof. Paper #1360

Gutierrez C, Singh SK (1992) A site effect study in Acapulco, Guerrero, Mexico: comparison of results from strong-motion and microtremor data. Bull Seismol Soc Am 82:642–659

ICC-IBC (2006) International building code, structural and fire-and life-safety provisions (seismic, wind, accessibility, occupancy and roof codes). Whittier, CA

Joyner WB, Fumal TE (1984) Use of measured shear-wave velocity for predicting geologic and site effects on strong ground motion. Proceedings of 8th World Conference on Earthquake Engineering, 2:777–784

Kagami H, Duke CM, Liang GC, Ohta Y (1986) Observation of 1- to 5-second microtremors and their application to earthquake engineering. Part II. Evaluation of site effect upon seismic wave amplification deep soil deposits. Bull Seismol Soc Am 72:987–998

Kanamori H (1986) Rupture process of subduction-zone earthquakes. Ann Rev Earth Planet Sci 14:293–322

Katz LJ (1976) Microtremor analysis of local geological conditions. Bull Seismol Soc Am 66:45–60

Katz LJ, Bellon RS (1978) Microtremor site analysis study at Beatty, Nevada. Bull Seismol Soc Am 68:757–765

Konno K, Ohmachi T (1998) Ground-motion characteristics estimated from spectral ratio between horizontal and vertical components of microtremors. Bull Seismol Soc Am 88:228–241

Lachet C, Bard PY (1994) Numerical and theoretical investigations on the possibilities and limitations of the Nakamura's technique. J Phys Earth 42:377–397

Lermo J, Chavez-Garcia FJ (1993) Site effect evaluation using spectral ratios with only one station. Bull Seismol Soc Am 83:1574–1594

Lermo J, Chavez-Garcia FJ (1994) Are microtremors useful in site response evaluation? Bull Seismol Soc Am 84:1350–1364

Malagnini L, Tricarico P, Rovelli A, Herrmann RB, Opice S, Biella G, de Franco R (1996) Explosion, earthquake, and ambient noise recording in a pliocene sediment-filled valley: inferences on seismic response properties by reference- and non-reference-site techniques. Bull Seismol Soc Am 86:670–682

Mucciarelli M (1998) Reliability and applicability of Nakamura's technique using microtremors: an experimental approach. J Earthq Eng 4:625–638

Mucciarelli M, Contri P, Mochavesi G, Cavano G, Gallipoli MR (2001): An emperical method to assess the seismic vulnerability of existing buildings using HVSR technique. Pure Appl Geophyscis 158:2635–2647

Nakamura Y (1989) A method for dynamic characteristics estimation of subsurface using microtremor on the ground surface. QR RTRI 30(1):25–33

Nakamura Y (1996) Real-time information systems for hazards mitigation. Proceedings of the 11th World Conference on Earthquake Engineering, Acapulco, Mexico. Paper No. 2134

Ohmachi T, Nakamura Y, Toshinawa T (1991) Ground motion characteristics of the San Francisco bay area detected by microtremor measurements. 2nd International conference on recent advances in geotechnical earthquake engineering and soil dynamics, St. Louis, Missouri, 1643–1648

Ohta Y, Kagami H, Goto N, Kudo K (1978) Observation of 1- to 5-second microtremors and their application to earthquake engineering. Part I: comparison with long period accelerations at the Tokachi-Oki earthquake of 1968. Bull Seismol Soc Am 68: 767–779

Park S, Elrick S (1998) Predictions of shear wave velocities in southern California using surface geology. Bull Seismol Soc Am 88:677–685

Parolai S, Bormann P, Milkereit C (2002) New relationship between VS, thickness of sediments, and resonance frequency calculated by the H/V ratio of seismic noise for the Cologne area (Germany). Bull Seismol Soc Am 92(6):2521–2527

SESAME European Project (2004) Guidelines for the implementation of the H/V spectral ratio technique on ambient vibrations measurements, processing and interpretation. WP12-Deliverable D23.12

Teves-Costa, Matias PL, Bard PY (1996) Seismic behavior estimation of thin alluvium layers using microtremor recordings. Soil Dyn Earthq Eng 15:201–209

Theodulidis N, Bard PY, Archuleta R, Bouchon M (1996) Horizontal-to-vertical spectral ratio and geological conditions: the case of Garner valley downhole in Southern California. Bull Seismol Soc Am 68: 767–779

Tinsley JC, Fumal TE (1985) Mapping Quaternary sedimentary deposits for areal variations in shaking response. US Geol Surv Prof Pap 1360:101–126

Wakamatsu K, Yasui Y (1996) Possibility of estimation for amplification characteristics of soil deposits based on ratio of horizontal to vertical spectra of microtremors. Proceedings of the 11th World Conference on Earthquake Engineering Acapulco. Mexico. Geophys Prospect 30:55–70

Weijermars R (1999) Surface geology, lithostratigraphy, and Tertiary growth of the Dammam dome, Saudi Arabia. A new guide. GeoArabia 4(2):199–266

Wills CJ, Petersen M, Bryant WA, Reichle M, Saucedo GJ, Tan S, Taylor G, Treiman J (2000) A site-conditions map for California based on geology and shear-wave velocity. Bull Seismol Soc Am 90:S187–S208